Geoscience Frontiers 6 (2015) 175–190

HOSTED BY

Contents lists available at ScienceDirect

China University of Geosciences (Beijing)

Geoscience Frontiers

journal homepage: www.elsevier.com/locate/gsf

Research paper

Main deposit styles and associated tectonics of the West Junggar region, NW China

Ping Shen[a,*], Hongdi Pan[a,b], Yuanchao Shen[a], Yuhong Yan[a], Shihua Zhong[a]

[a] Key Laboratory of Mineral Resources, Institute of Geology and Geophysics, Chinese Academy of Sciences, Beijing 100029, China
[b] College of Earth Sciences, Chang'an University, Xi'an 710054, China

ARTICLE INFO

Article history:
Received 2 December 2013
Received in revised form
3 May 2014
Accepted 13 May 2014
Available online 27 May 2014

Keywords:
Mineral deposit styles
Metallogenic belts
Tectonic-mineralized epoch
West Junggar
Xinjiang

ABSTRACT

The West Junggar region, located in the loci of the Central Asian Orogenic Belt, is a highly endowed metallogenic province with >100 tonnes Au, >0.7 Mt Cu, >0.3 Mt Mo, and >2.3 Mt chromite as well as significant amounts of Be and U. The West Junggar region has three metallogenic belts distributed systematically from north to south: (1) late Paleozoic Saur Au-Cu belt; (2) early Paleozoic Xiemisitai-Sharburt Be-U-Cu-Zn belt; (3) late Paleozoic Barluk-Kelamay Au-Cu-Mo-Cr belt. These belts host a number of deposits belonging to at least eight economically important styles, including epithermal Au, granite-related Be-U, volcanogenic massive sulfide (VMS) Cu-Zn, podiform chromite, porphyry Cu, hydrothermal quartz vein Au, porphyry-greisen Mo(-W), and orogenic Au. These deposit styles are associated with the tectonics prevalent during their formation. Five tectonic-mineralized epochs can be recognized: (1) Ordovician subduction-related VMS Cu-Zn deposit; (2) Devonian ophiolite-related podiform chromite deposit; (3) early Carboniferous subduction-related epithermal Au and porphyry Cu deposits; (4) late Carboniferous subduction-related granite-related Be-U, porphyry Cu, and hydrothermal quartz vein Au deposits; and (5) late Carboniferous to early Permian subduction-related porphyry-greisen Mo(-W) and orogenic Au deposits.

1. Introduction

The Central Asian Orogenic Belt (CAOB) is one of the largest orogenic collages in the world (Sengör et al., 1993; Jahn et al., 2000, 2004; Windley et al., 2007; Xiao et al., 2008, 2009, 2010a, 2013; Santosh and Kusky, 2010; Kröner et al., 2013, 2014; Xiao and Santosh, 2014). The West Junggar region in Xinjiang (NW China) is located in the loci of the CAOB (Fig. 1A) and is bounded by the Altai orogen to the north and by the Tianshan orogen to the south, and it extends westward to the Junggar-Balkhash region in adjacent Kazakhstan and eastward to the Junggar Basin in Xinjiang, China (Fig. 1B). It is a highly endowed metallogenic province in the CAOB with >100 tonnes Au, >0.7 Mt Cu, >0.3 Mt Mo, and >2.3 Mt chromite as well as significant amounts of Be and U. It hosts many mineral deposits, such as Baiyanghe Be-U deposit, Kurzhenkuola, Kuogesay and Hatu Au deposits, Hongguleleng Cu-Zn deposit, Sartuohai chromite deposit, Baogutu Cu deposit, and Suyunhe and Hongyuan Mo(-W) deposits (Shen et al., 1993; Zhou et al., 2001; Wang et al., 2005, 2006; Yuan et al., 2006; Zhou et al., 2006, 2008; Zhu and Xu, 2006; Song et al., 2007; An and Zhu, 2010; Shen et al., 2010a,b; Tan and Zhu, 2010; Wei and Zhu, 2010; Pirajno et al., 2011; Wang et al., 2012; Zhang and Zhang, 2014). The spatial and temporal distribution of these deposits relates to their formation within a unique tectonic framework.

In this article we identify three metallogenic belts and describe the selected deposits of the West Junggar region using published literature and our own field observations. We also review the relationship between the deposits' metallogenesis and the tectonic settings and discuss models that attempt to explain the links of these deposits to aspects of the geodynamic evolution of the West Junggar region.

* Corresponding author. Tel.: +86 10 82998189; fax: +86 10 62010846.
E-mail address: pshen@mail.iggcas.ac.cn (P. Shen).

Peer-review under responsibility of China University of Geosciences (Beijing)

http://dx.doi.org/10.1016/j.gsf.2014.05.001
1674-9871/

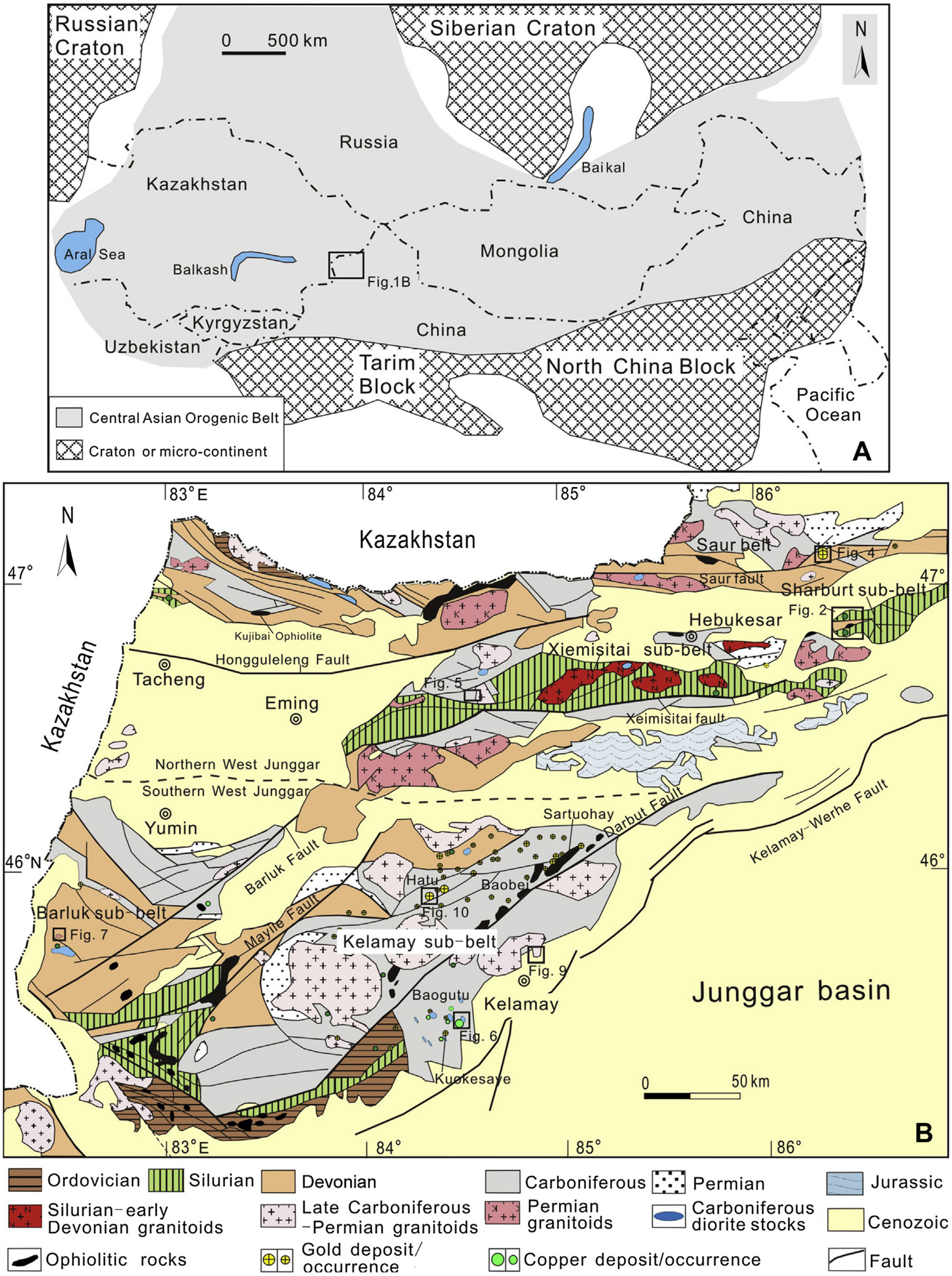

Figure 1. (A) Location of the study area in the Central Asian Orogenic Belt (modified after Jahn et al., 2000; Xiao et al., 2008, 2009). (B) Geological map of the West Junggar (modified after Shen et al., 1993; Chen et al., 2010; Shen et al., 2012a).

2. Geological outline

The West Junggar region has several mountains (Fig. 1B). The Saur, Tarbahatai, Xiemisitai, and Sharburti mountains are approximately E-trending in the northern part of the West Junggar region. The Barluke mountains and Kelamay region are mainly NE-trending in the southern part of the West Junggar region.

Geologically, in the northern part of the West Junggar region, the late Paleozoic volcanic rocks exclusively outcrop in the Saur mountains and the early Paleozoic volcanic rocks are confined to the Xiemisitai and Sharburt mountains (Fig. 1B). Strata from Ordovician to Permian are well-exposed (Zhu and Xu, 2006; Shen et al., 2008, 2012a; Zhou et al., 2008). In the southern part of the West Junggar region, the late Paleozoic volcanic rocks exclusively outcrop in the Barluke mountains and Kelamay region (Shen et al., 1993; Wang et al., 2004; Geng et al., 2009, 2011; Tang et al., 2009, 2010; Zhang et al., 2011).

Structurally, the northern part of the West Junggar region is characterized by several E-trending faults including the Saur, Hongguleleng and Xiemisitai faults (Fig. 1B). This is very different from the southern part of the West Junggar region where the major faults are NE-trending faults including the Barluk, Mayile, and Darbut faults (Fig. 1B).

Plutons occurring in the West Junggar region (Fig. 1B) include late Silurian–early Devonian (ca. 422 to 405 Ma; Chen et al., 2010), early Carboniferous (ca. 346 to 321 Ma; Han et al., 2006; Zhou et al., 2006, 2008), late Carboniferous (ca. 319 to 312 Ma; Jahn et al., 2000; Chen and Jahn, 2004; Han et al., 2006; Yuan et al., 2006; Tang et al., 2009; Shen et al., 2012b), and the latest late Carboniferous–middle Permian (ca. 304 to 263 Ma; Shen et al., 1993; Han et al., 2006; Zhou et al., 2008) granitoids, determined on the basis of secondary ion mass spectrometry (SIMS), sensitive high resolution ion microprobe (SHRIMP), and laser ablation inductively coupled plasma mass spectrometry (LA-ICP-MS) zircon U-Pb ages. The late Silurian–early Devonian granitoids mainly occur in the Xiemisitai Mountains, the early Carboniferous granitoids in the Saur mountains, and the late Carboniferous granitoids in the Barluk mountains and the Kelamay region (Fig. 1B). By contrast, the latest late Carboniferous–middle Permian plutons occur in the Saur, Xiemisitai, Barluk, and Kelamay regions, suggesting that these plutons occur across the different tectonic units of the West Junggar region (Fig. 1B).

3. Metallogenic belts and tectonic setting

The West Junggar region hosts many mineral deposits, which commonly form well defined metallogenic belts, such as the Saur, Xiemisitai-Sarburt, and Barluk-Kelamay belts from north to south. The Saur and Xiemisitai-Sarburt belts, separated by the Hebukesar depressed area, are located in the northern West Junggar region, and the Barluk-Kelamay belt is located in the southern West Junggar region (Fig. 1B). An overview of the distribution of metallogenic belts in the West Junggar region is given in Fig. 1B.

The Saur belt extends in an E–W direction for about 100 km and contains epithermal Au and porphyry Cu deposits (Shen et al., 2008; Zhou et al., 2008; Yin et al., 2009; Guo et al., 2010). The Xiemisitai-Sharbut belt that extends in an E–W direction for about 250 km, is 20 km wide, and contains granite-related Be-U (Wang et al., 2012; Zhang and Zhang, 2014), volcanic-hosted Cu (Shen et al., 2010a,b), and Cu-Zn deposits (Shen et al., 2014). The Barluk-Kelamay belt includes the Barluk sub-belt and Kelamay sub-belt, separated by the Mayile Fault (Shen et al., 2013a, b). The Barluk sub-belt, an NE-trending belt, has porphyry Cu (Shen et al., 2013a) and porphyry-greisen Mo(-W) deposits. The Kelamay sub-belt (including the Hatu, Sartuohai, and Baogutu areas) is the most important belt of the West Junggar region and hosts hydrothermal Au (Shen et al., 1993; Wang et al., 2005, 2006; Zhu and Xu, 2006; An and Zhu, 2010), podiform chromite (Zhou et al., 2001; Tan and Zhu, 2010), porphyry Cu (Song et al., 2007; Shen et al., 2010a,b), and porphyry-greisen Mo deposits (Shen et al., 2013b). Each of these metallogenic belts is associated with the tectonics prevalent during their formation.

3.1. Late Paleozoic Saur metallogenic belt

A suite of Devonian and Carboniferous volcano-sedimentary strata continuously extends from the Saur mountains to Wulungu Lake (Fig. 1B; Liu et al., 2003). They are the middle Devonian Saurshan Group and the lower Carboniferous Heishantou Group. The former consists of intermediate-felsic volcanic rocks, volcaniclastic rocks, and basaltic lavas. The latter consists of a succession of mafic to intermediate volcanic rocks and volcaniclastics with intercalations of siltstone and limestone. These Devonian and Carboniferous sequences are intruded by Carboniferous and Permian intrusions (Zhou et al., 2008; Guo et al., 2010).

The Saur mountains are characterized by volcanic complexes that host epithermal gold deposits (Shen et al., 2007, 2008; Zhou et al., 2008). The volcanic complex consists of mafic to intermediate volcanic rocks and volcaniclastics of the lower Carboniferous Heishantou Group. The volcanic rocks have a transitional character from calc-alkaline to tholeiite and range from porphyritic basalts, basaltic andesites, and andesites to dacites with high $\varepsilon_{Nd}(t)$ (+3.5 to +4.7) values (Shen et al., 2008). These volcanic rocks formed in an island arc. Early Carboniferous intrusions host porphyry Cu deposits (Guo et al., 2010). These ore-bearing intrusive rocks are enriched in light rare earth elements (LREE) and large-ion lithophile elements (LILE) with negative Nb anomaly and positive $\varepsilon_{Nd}(t)$ (+6.7 to +7.5), suggesting that they were generated in an island arc (Guo et al., 2010). Therefore, the Saur metallogenic belt occurred in an early Carboniferous island arc.

3.2. Early Paleozoic Xiemisitai-Sharburt metallogenic belt

The Xiemisitai-Sharburt metallogenic belt includes the Xiemisitai and Sharburt sub-belts from west to east.

3.2.1. Xiemisitai metallogenic sub-belt

The Xiemisitai sub-belt is characterized by late Silurian–early Devonian volcanic complexes (Shen et al., 2012a). These volcanic rocks are intruded by late Silurian–early Permian granites (Zhou et al., 2008; Chen et al., 2010). The Xiemisitai Cu deposit is hosted in the late Silurian–early Devonian volcanic complexes. The Baiyanghe Be-U deposit is associated with late Carboniferous granite porphyry.

The Xiemisitai volcanic complexes consist of volcanic rocks and subvolcanic units. The former include andesite, rhyolite, and their pyroclastic equivalents. The latter are felsite and granite porphyry. Andesite is moderately LREE-enriched, with a marked negative Nb anomaly. Rhyolite, felsite and granite porphyry are enriched in LREE and depleted Nb. Their $\varepsilon_{Nd}(t)$ values range from +0.19 to +1.88. Therefore, the Xiemisitai complexes were formed in an island arc setting (Shen et al., 2012a).

Zhang and Zhang (2014) have suggested that the Baiyanghe granite porphyry is A-type granite and can be classified into A_1 group. Positive values of $\varepsilon_{Nd}(t)$ (+4.06 to +5.29) and high concentrations of incompatible elements suggest that the granite porphyry has been derived from an oceanic island basalt-like mantle source. Characterized by the features of within-plate granites, a back-arc basin tectonic setting is favored for the petrogenesis of the Baiyanghe granite porphyry. Such a setting indicates that the subduction of the Irtysh-Zaysan oceanic lithosphere beneath the Saur arc was still active during the late Carboniferous.

3.2.2. Sharburt metallogenic sub-belt

The Sharburti sub-belt includes intermediate-basic volcanic rocks from the Ordovician to Silurian age. The Hongguleelng Cu-Zn deposit occurred in the middle Ordovician Bulukeqi Group of intermediate-basic volcanic rocks. These volcanic rocks include basalt, andesite, and their pyroclastic equivalents. We divided these volcanic rocks into two types (Shen et al., 2014). Type I lavas are Nb-enriched basalts (NEB; Nb = 14–15 ppm) and come from mantle metasomatized by slab melts. Type II lavas are tholeiitic to calc-alkaline and calc-alkaline basalts and andesite's; their $\varepsilon_{Nd}(t)$ values range from +1.5 to +4.5, suggesting that they were generated in an island arc setting. Contemporary tholeiitic to calc-alkaline basalt-andesite and Nb-enriched basalt association suggest a model of intra-oceanic subduction influenced by ridge subduction during the Ordovician Period (Shen et al., 2014).

3.3. Late Paleozoic Barluk-Kelamay metallogenic belt

The Barluk-Kelamay metallogenic belt, located in the southern West Junggar, includes Barluk and Kelamay sub-belts from west to east.

3.3.1. Barluk metallogenic sub-belt

The Barluk metallogenic sub-belt has developed Suyunhe Mo(-W) deposit and Jiamantieliek Cu deposit. The volcano-sedimentary strata of the middle Devonian Barluk and Tielieked Groups occur widely in the Barluk mountains close to the China–Kazakhstan border. These Devonian sequences are intruded by Carboniferous–Permian intrusions. The Jiamantielieke Cu and Suyunhe Mo(-W) deposits are associated with these intrusions.

The Jiamantieliek ore-bearing intrusion is a calc-alkaline intermediate intrusion which comprises main-stage diorite stock and minor late-stage diorite porphyry dikes. They are enriched in LREE and LILE with a negative Nb anomaly and positive $\varepsilon_{Nd}(t)$ (+1.6 to +3.4), suggesting that they were generated in an island arc (Shen et al., 2013a).

The Suyunhe granites are alkali granites characterized by alkali and Fe enrichment. Because of their high $\varepsilon_{Nd}(t)$ values (+3.39 to +3.74), the alkali granites are considered to have been derived from a juvenile lower crust (Shen et al., 2013b).

3.3.2. Kelamay metallogenic sub-belt

The Kelamay metallogenic sub-belt includes the Hatu area in the northern part of the Darbut Fault and the Baogutu area in the southern part of Darbut Fault. The Darbut Fault is a major sinistral NE-trending fault zone. Associated with the Darbut Fault is a melange zone where Sartuhai chromite deposits occur.

Most gold deposits of the Kelamay metallogenic sub-belt occur in the Hatu area and are hosted in the early Carboniferous Baogutu Group. They could be associated with the early Permian granite (Li et al., 2000). Granitic intrusions are pervasively developed in the Kelamay region (Fig. 1B). Because most plutons are undeformed and alkaline enriched, they have been envisaged as post-collisional granites derived either from a long-lived depleted mantle reservoir (Han et al., 2006) or from a Paleozoic juvenile basaltic lower crust (e.g. Hu et al., 2000; Chen and Arakawa, 2005). Most recently, some researchers consider that a ridge subduction model could account for the formation of these granitoids (Geng et al., 2009; Tang et al., 2010; Yin et al., 2010; Zhang et al., 2011). These results suggest that subduction was ongoing in the late Carboniferous and possibly in the Permian period.

Most intrusion-related Cu, Au, and Mo deposits of the Kelamay metallogenic sub-belt occur in the Baogutu area. The Baogutu porphyry Cu deposit is associated with the late Carboniferous diorite (named Baogutu V stock). Although the Kuogesay Au deposit is hosted in the tuff of the early Carboniferous Baogutu Group, it is associated with late Carboniferous diorite (named Baogutu IV stock). The Hongyuan Mo deposit is associated with the late Carboniferous–early Permian granite.

The Baogutu ore-bearing intrusions (including Baogutu IV and V stocks) are calc-alkaline intermediate intrusions. They are enriched in LREE and LILE with a negative Nb anomaly. Their isotopic composition ($\varepsilon_{Nd}(t) = +4.4$ to +6.0) shows a depleted mantle source. These features suggest they were generated in an island arc (Zhang et al., 2006; Shen et al., 2009; Wei and Zhu, 2010). Our unpublished data suggests that the Hongyuan ore-bearing intrusion is alkaline garnite. More recently, some researchers have considered that the Carboniferous Junggar Ocean may have been subducting north-westward beneath the Kelamay arc in the Carboniferous (Tang et al., 2009, 2010; Geng et al., 2009, 2011; Yin et al., 2010; Yang et al., 2012). Zhang et al. (2011) proposed that there were double subduction systems in the Darbut area in the Carboniferous. Our study about the Carboniferous volcanic rocks and intrusions in the Kelamay region supported the double directed subduction model (Shen et al., 2013a,c).

Sartuhai podiform chromite deposits and occurrences are found in the Darbut ophiolitic belt, which consists mainly of mantle peridotites and lavas. The Sartuohai podiform chromite deposit is related to ophiolite (Zhou et al., 2001; Tan and Zhu, 2010). The Devonian lavas of the Darbut ophiolite generally outcrop as blocks in a matrix of ultramafic rocks and/or mudstone (Zhang et al., 2011). They have a depleted LREE and mid-oceanic ridge basalt (MORB)-like signature with a small negative Nb anomaly, suggesting they were formed in a back-arc basin (Zhang et al., 2011).

4. Main deposit styles

The West Junggar region hosts many mineral deposits (Table 1). The following is a review of the eight main deposit types within the West Junggar region covered in chronological order (see Section 4.1 for detail) of formation: (1) Ordovician volcanogenic massive sulfide (VMS) Cu-Zn deposit (e.g. Honggulelengg); (2) Devonian podiform chromite deposit (e.g. Sartuohai); (3) early Carboniferous epithermal gold deposit (e.g. Kuoerzhenkuola); (4) late Carboniferous granite-related Be-U deposit (e.g. Baiyanghe); (5) late Carboniferous porphyry Cu deposit (e.g. Baogutu); (6) late Carboniferous hydrothermal quartz vein Au deposit (e.g. Kuogesay); (7) late Carboniferous–early Permian porphyry-greisen Mo(-W) deposit (e.g. Suyunhe, Hongyuan); and (8) early Permian orogenic Au deposits (e.g. Hatu).

4.1. Ordovician VMS Cu-Zn deposit

The Hongguleleng deposit or occurrence, located in the Sharburt Mountains (Fig. 1B), is a newly-discovered Cu-Zn deposit. It is hosted in the mafic volcanic rocks of the middle Ordovician Bulukeqi Group. Our previous work has suggested it is a volcanic-hosted Cu-Zn deposit, based on the characteristics of the deposit geology and host rocks (Shen et al., 2014). In this study, we consider it to be a VMS deposit based on the newly-discovered massive ores in this deposit.

The fossil-dated middle Ordovician Bulukeqi Group occurs in the Hongguleleng ore district and consists of two stratigraphic subgroups: (1) the lower group consists of a succession of basalt, andesite, and brecciated andesite intercalated with andesitic tuff; (2) the upper group is characterized by andesite and andesitic tuff intercalated with greywacke. Mineralization is generally hosted by the lower group of the Bulukeqi Group (Fig. 2). The ore district includes NE-striking faults, with minor NW-striking faults.

Two mineralized zones have been identified within a 2.2 km × 1.8 km area of the Hongguleleng ore district. They are the north and south zones and are controlled by regional NE-trending faults. Orebodies of the two mineralized zones are spatially associated with the NE-trending faults. NW-trending faults are mineralized or contain economic mineralization. The local geology team identified ten orebodies in the north zone and four orebodies in the south zone. The dimensions of the orebodies are highly variable; generally they range from 10 to 100 m long and 0.5 to 5 m thick at the surface. Wall-rock alteration associated with this mineralization has resulted in the development of chlorite, pyrite, carbonate, quartz, sericite, and epidote alteration.

Table 1
U-Pb zircon ages of the ore-bearing intrusions and Re-Os ages of molybdenites from the West Junggar terrain.

Deposits	Deposit types	Dated minerals/ rocks	Dating methods	Ages (Ma)	Data sources	Reserves	Data sources
Saur							
Kurzhenkula	Epithermal gold	Fluid inclusions of auriferous quartz vein	^{40}Ar-^{39}Ar plateau	332 ± 22	Shen et al., 2007, 2008	11.7 t Au (average grade 6.02 g/t)	Shen et al., 2007
		Andesite	Rb-Sr isochron	343 ± 22	Liu et al., 2003		
Xiemisitai-Sarburt							
Hongguleleng	VMS copper	Volcanic rocks	Fossil-dated	Middle Ordovician	BGMRXUAR, 1993	–	
Baiyanghe	Granite-related Be-U	Granite	LA-ICP-MS U-Pb	313.4 ± 2.3	Zhang and Zhang, 2014		
Barluk							
Jiamantieliek		Diorite	SHRIMP U-Pb	313.0 ± 2.2	Shen et al., 2013a	–	
		Diorite porphyry	SHRIMP U-Pb	312.3 ± 2.2	Shen et al., 2013a		
Suyunhe		Granite	Re-Os	300.7 ± 4.1	Shen et al., 2013b	27 × 10^4 t	Zheng, 2013 private communications
Kelamay							
Sartohay	Chromite	Gabbros	LA-ICP-MS	391 ± 7	Gu et al., 2009	64.35 × 10^4 t	http://www.xjdk.net
		Basalt	Rb-Sr isochron	411 ± 18	Li and Chen, 2004		
Baogutu	Porphyry copper	Diorite	SIMS U-Pb	313.0 ± 2.2	Shen et al., 2012b	63 × 10^4 t Cu (average grade 0.28%)	Shen et al., 2010a
		Diorite porphyry	SIMS U-Pb	312.3 ± 2.2	Shen et al., 2012b		
		Molybdenite	Re-Os isochron	312.4 ± 1.8	Shen et al., 2012b		
			Re-Os isochron	310 ± 3.6	Song et al., 2007		
Kuogesay	Diorite-related gold	Diorite	SHRIMP U-Pb	309.9 ± 1.9	Tang et al., 2009	6.05 t Au (average grade 2%)	http://www.xjdk.net
		Auriferous quartz vein	Rb-Sr isochron	311 ± 10	Li et al., 2000		
Hongyuan	Granite-related Mo	Granite	LA-ICP-MS U-Pb	302	Li et al., 2012	–	
			Re-Os isochron	294.6	Li et al., 2012		
			Re-Os isochron	314	Yan et al., 2014		
Hatu	Hatu (Qiqiu I)	Tuff	SHRIMP U-Pb	328.1 ± 1.8	Wang and Zhu, 2007	56 t Au (average grade 4.99%)	Xiao et al., 2010a,b
		Tuff	SIMS U-Pb	324.0 ± 2.8 ~324.9 ± 3.4	Shen et al., 2013c		
		Basalt	Rb-Sr isochron	328 ± 31Ma	Li and Chen, 2004		
		auriferous quartz vein	Rb-Sr isochron	290 ± 5	Li et al., 2000		
	Qiqiu II	auriferous quartz vein	Rb-Sr isochron	289 ± 29	Li et al., 2000	15.87 t Au (average grade 2.00 g/t)	http://www.dynastygoldcorp.com/s/Project_Hatu.asp

The mineralization is hosted by basalt and andesite. The ores include amygdales, breccia, band, dense disseminated, and massive ores (Fig. 3). The amygdales are filled by chalcopyrite. Metallic minerals in ore assemblages include pyrite, chalcopyrite, and minor sphalerite and galena. Gangue minerals are chlorite, carbonate, quartz, sericite, and epidote.

4.2. Devonian podiform chromite deposit

Many podiform chromite deposits and occurrences are found in the Darbut ophiolitic belt in the Kelamay region. They include 14 orebody groups that consist of 563 orebodies (Zhang et al., 2009). The local geology team reported that these orebodies have a resource of 229.3 × 10^4 tonnes ore. The Sartuohai is the largest of these; it is also the second largest chromite deposit in China (Zhang et al., 2009).

The Darbut ophiolite belt consists mainly of mantle peridotites and lavas. The peridotites outcrop in a narrow belt extending about 20 km in an NE–SW direction and have an exposed area of about 20 km^2. The Sartuohai deposit is located in the eastern part of the Darbut ophiolitic belt and is a typically high-Al podiform chromite deposit related to ophiolite (Zhou et al., 2001; Tan and Zhu, 2010).

The Sartuohai deposit is characterized by No. 26 orebody group that includes five orebodies. The No. 1 orebody is the largest; it is 160 m long, 110 m deep, and 8.54–42.7 m thick. The local geology team reported that the No. 26 orebody group contains 64.35 × 10^4 tonnes of ore (Table 1). The orebody is hosted in harzburgite, although they are typically enveloped by dunite. The chromitite bodies are mainly tabular or lensoid in form, but some occur as veins, fracture fillings, and linear or planar segregations (Zhou et al., 2001). The orebodies are composed of massive and disseminated ores as well as their transitional types. The wall-rock alteration is extensive serpentinite alteration. The mineral assemblage in the ore and wall rock (dunite) is pentlandite-heazlewoodite-millerite-maucherite and heazlewoodite-pentlandite-maucherite, respectively (Tan and Zhu, 2010).

4.3. Early Carboniferous epithermal Au deposit

The late Paleozoic volcanic rocks occur in the Saur mountains. A close spatial and temporal relationship exists between the volcanic rocks and hydrothermal gold mineralization in the Saur mountains (Yuan et al., 2006; Shen et al., 2007, 2008; Zhou et al., 2008; Yin et al., 2010). The intermediate to silicic volcanic rocks and/or caldera fracture systems host a number of gold deposits. The Kuoerzhenkuola, located in the eastern part of the Saur mountains, is the largest (Fig. 1B). This deposit has proven resources of 11.7 t of gold at an average grade of 6.02 g/t (Table 1). Our previous works

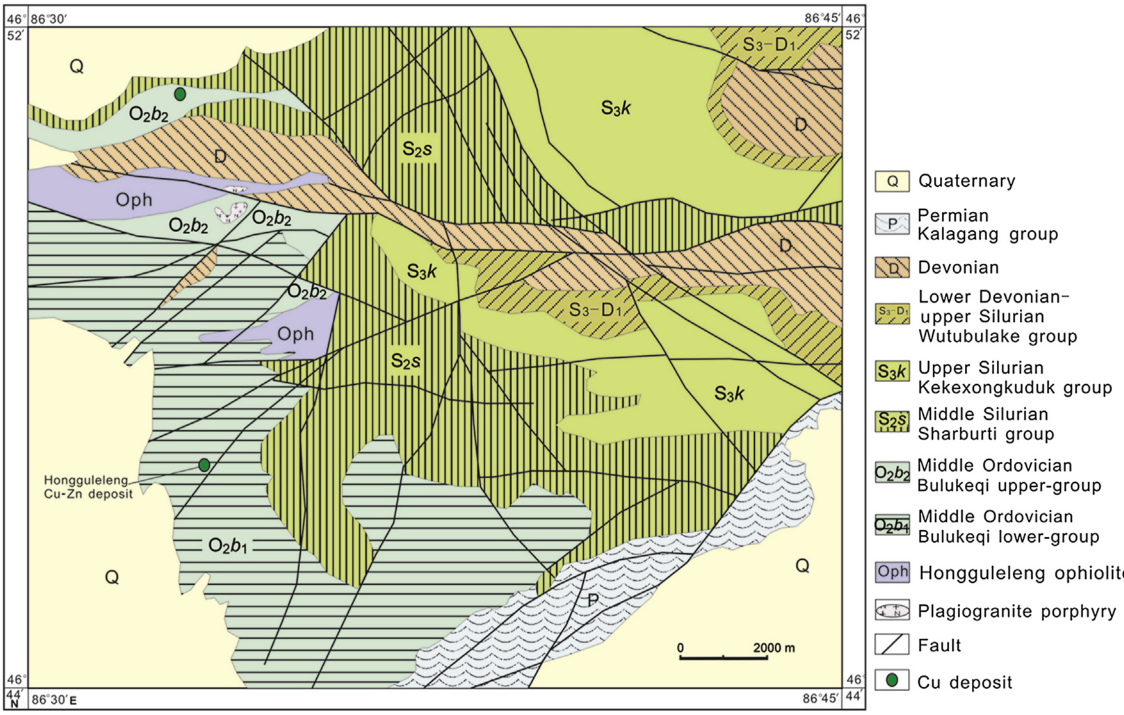

Figure 2. Geological map of the Sharburt mountains in the northern West Junggar (modified after BGMRXUAR, 1993; Shen et al., 2014).

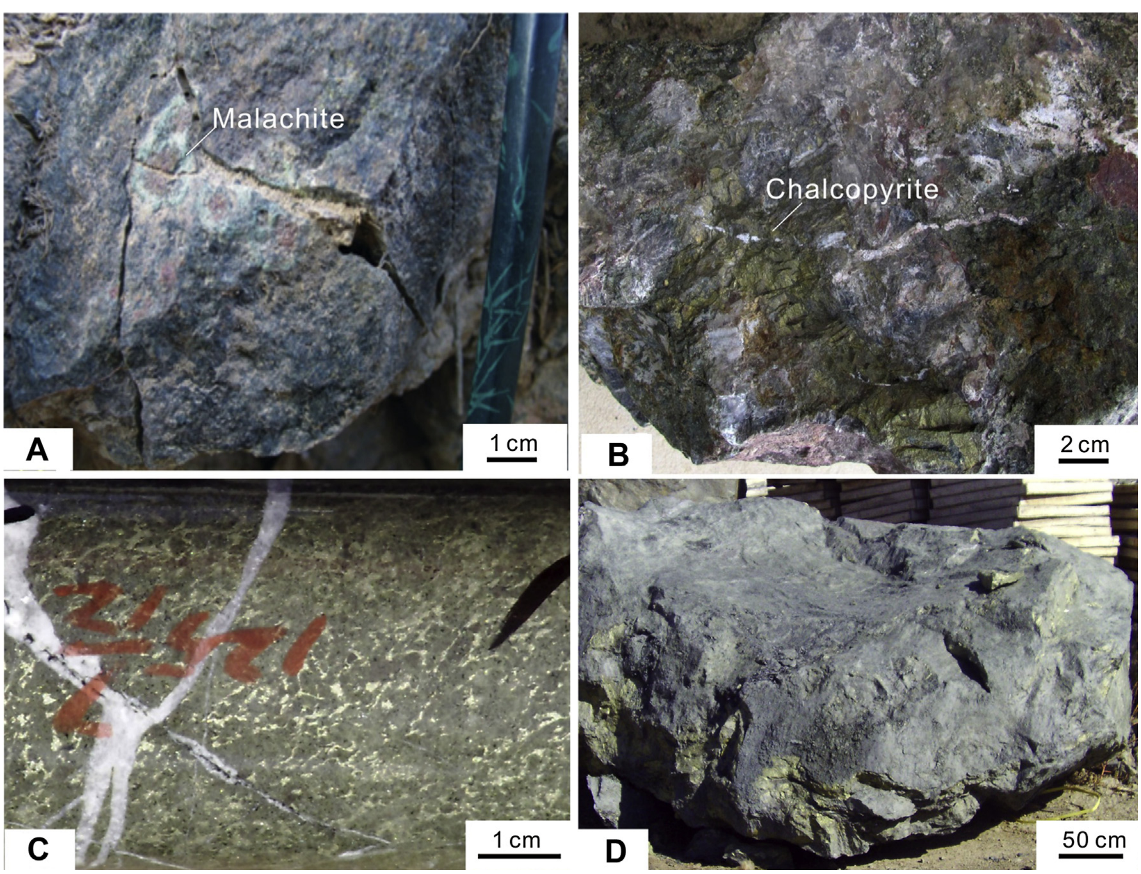

Figure 3. Photographs of the main ores from the Hongguleleng Cu-Zn deposit. (A) Ore with amygdales structure; (B) ore with band structure; (C) ore with dense disseminated and massive structure; (D) ore with massive structure.

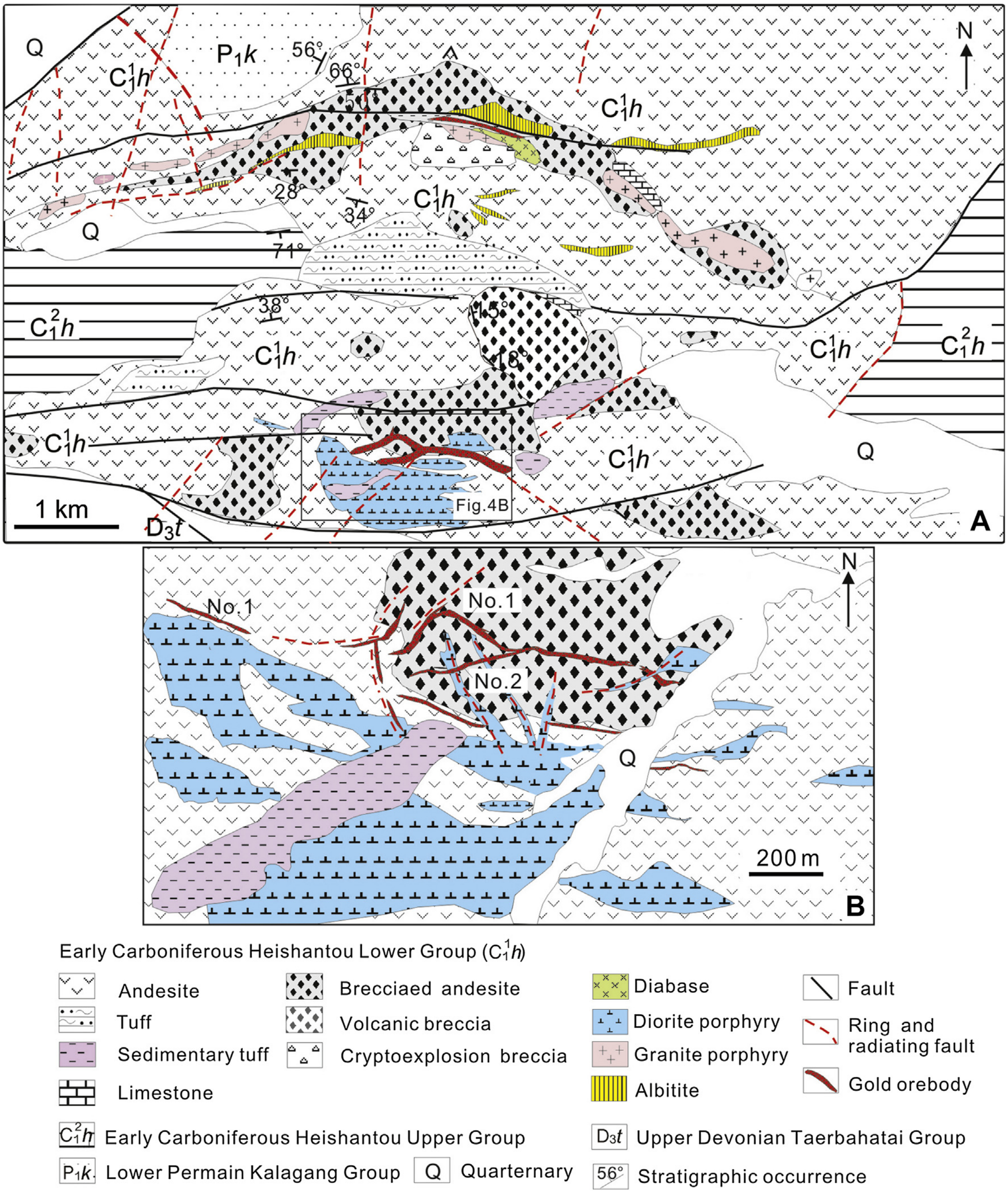

Figure 4. (A) Geological map of the caldera complex in the Saur mountains, showing location of gold deposit. (B) Geological map of the Kuoerzhenkuola gold deposit (Shen et al., 2008).

considered it to be a high sulphidation-style epithermal Au deposit based on the strong kaolinitization and alunitization alteration as well as the close relationship between the volcanic activity and gold mineralization (Shen et al., 2007, 2008).

The early Carboniferous Heishantou Groups occur in the Kuoerzhenkuola ore district (Fig. 4A). They consist of andesite, andesite porphyry, brecciaed andesite, sandstone, siltstone, mudstone, and limestone. Late Paleozoic granodiorites, granites, diorite porphyries, albite-porphyry dykes, and breccia pipes are widely developed. The main structures are ENE-trending folds and major E-trending and minor NE-and NW-trending faults.

Five Au-bearing alteration zones are controlled by E-trending faults and are hundreds to thousands of meters long and 10–30 m wide. Hydrothermal alteration includes kaolinitization, silicification, sericitization, chloritization, epidotization, alunitization, and fluoritization. All the gold orebodies are contained within these alteration zones. The largest orebody (orebody No. 1; Fig. 4B) is 1700 m long and 1.6–10 m wide, and it extends down dip to 380 m below the surface. Ore grades range from 2.6 to 79.1 g/t Au (average 7.28 g/t). There are two types of ore: (1) sulfide-quartz stockworks, disseminations, and breccias; (2) massive sulfide-quartz veins. The ore minerals are mainly pyrite, chalcopyrite, pyrrhotite, and native gold; whereas the gangue minerals include quartz, montmorillonite, kaolinite, chlorite, epidote, calcite, and alunite.

4.4. Late Carboniferous granite-related Be-U deposit

The Baiyanghe beryllium-uranium deposit, located in the western part of the Xiemisitai mountains (Fig. 1B), is one of the largest Be-U deposits in Asia (Wang et al., 2012).

In the Baiyanghe ore district, the stratigraphic sequence mainly includes the following: intermediate-acidic volcanic and pyroclastic rocks of the late Devonian Tarbagatay Group; limestone, conglomerate, siliceous shale, and mudstone of the early Carboniferous Hebukehe Group; basic-intermediate volcanic and pyroclastic rocks of the early Carboniferous Heishantou Group; and mudstone of the Neogene Taxihe Group (Fig. 5; Wang et al., 2012). The Baiyanghe Be-U deposit is associated with the Baiyanghe granite porphyry that outcrops over an 8 km × 2 km area and is about 130 m in thickness (Wang et al., 2012). The Baiyanghe granite porphyry was emplaced into the Devonian intermediate-acidic volcanic and pyroclastic rocks. The main orebodies occur in the contact zone of the granite porphyry and the wall rocks (Fig. 5). The wall rocks are volcanic lava or pyroclastic rocks which are from the upper Devonian and lower Carboniferous Periods (Zhang and Zhang, 2014).

The orebodies present themselves in bedded form and range from 600 to 800 m in depth and 0.69 to 28.89 m thick (Wang et al., 2012). The main beryllium mineral is bertrandite and main uranium mineral is pitchblende. The orebodies are associated with haematitization and fluoritization. The orebodies are affected by contact zone structure, and the essential factors in the formation of rich and big beryllium-uranium orebodies are multi-hydrothermal activity and multiphase superposition mineralization (Wang et al., 2012).

4.5. Late Carboniferous porphyry Cu deposit

Porphyry copper deposits are found in the southern part of the West Junggar region where Baogutu porphyry Cu deposit occur (Fig. 1B).

The Baogutu deposit is located about 60 km southwest of Kelamay City. It contains 0.63 Mt Cu metal at an average grade of 0.28%, 0.018 Mt Mo metal at an average grade of 0.011%, and 14 tonnes Au metal at an average grade of 0.1 ppm (Table 1). The mineralized intrusion (also called stock V) is intruded in the lower Carboniferous Baogutu and Xibeikulasi groups (Fig. 6A). The orebodies hosted in the mineralized stock and adjacent wall rocks occupy an area of 1100 m × 800 m and extend to a depth >800 m (Fig. 6B).

Our previous work has recognized two mineralized intrusive phases at Baogutu, which are the stage 1 diorite stock and stage 2 diorite porphyry dikes (Shen et al., 2010a,b). The stage 1 stock, comprised of dominant diorite and minor gabbro and tonalite (Shen and Pan, 2013), hosts the bulk of the Cu-Au-Mo mineralization at Baogutu (Fig. 6). They have been overprinted by three alteration assemblages, including early potassic assemblage, surrounding propylitic assemblage, and late phyllic alteration. Potassic alteration is associated with most Cu-Au mineralization and phyllic alteration is associated with most Cu-Mo mineralization. The dominant disseminated mineralization and lesser amounts of vein stockworks occur in Baogutu. The main mineral assemblages of the deposit are pyrite, chalcopyrite, pyrrhotite, and molybdenite. Most inclusions in quartz are rich in CH_4 (Shen et al., 2010b). The Baogutu porphyry Cu deposit has reduced mineralization features (Shen and Pan, 2013). It resulted from a significant country-rock contamination (including the reduced materials, e.g. carbonaceous sediment) after emplacement of the Baogutu magma (Shen and Pan, 2013).

4.6. Late Carboniferous hydrothermal quartz vein Au deposit

Many hydrothermal quartz vein Au deposits occur in the Kelamay region (Fig. 1B). The Kuogesay (also called Baogutu) deposit is the largest. It is 15 km SW of the Baogutu porphyry Cu deposit (see Fig. 1B) and occurs 1–2 km NE from a diorite intrusion (also called stock IV). The Kuogesay Au deposit is hosted within the tuff of the early Carboniferous Baogutu Group (Fig. 1B) and is a diorite-related hydrothermal Au deposit (Shen et al., 1993). This deposit has proven resources of 6 t of gold at an average grade of 2 g/t (Table 1).

Most of the Au-bearing quartz-sulfide veins are lensoid or ribbon-like in morphology, dipping to 301° to 328° at angles of 70° to 77°. Some veins reach 400 m in depth with lengths of 10 to 150 m and a planar thickness of 0.5 to 3 m. The grade of gold is highly variable; it seems to increase with depth (locally up to 100 g/t). More than 20 Au-bearing veins are exposed at surface, but current mining is focused on the buried lodes. The NNE-trending faults control the distribution of the Au-bearing quartz-sulfide veins and diorite dykes, while the E-trending faults cut through most of these veins and dykes (Shen et al., 1993; An and Zhu, 2010). An and Zhu (2010) detected the presence of Sb minerals (stibnite, ullmannite, tetrahedrite) as well as native As and Sb co-existing with chalcopyrite and pyrrhotite, or as isolated grains enclosed in calcite veins.

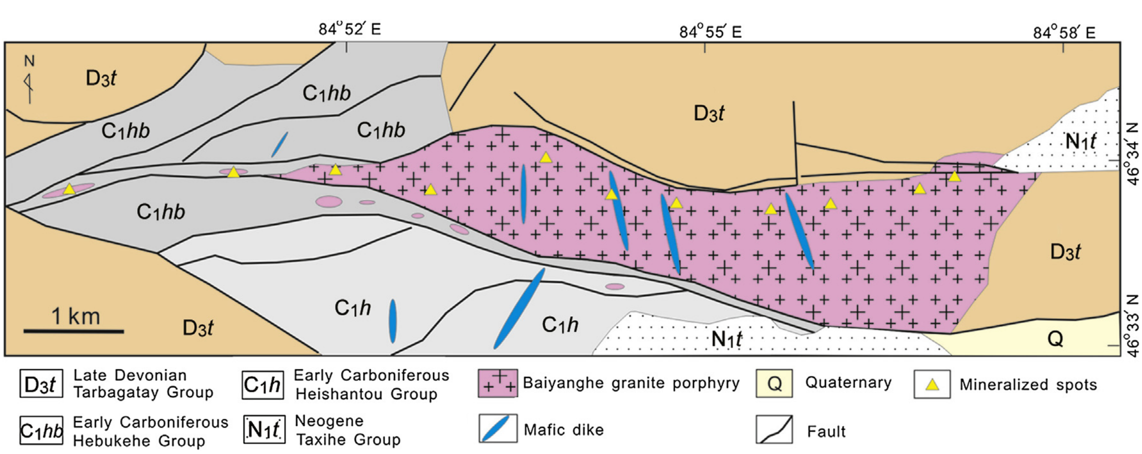

Figure 5. Geological map of the Baiyanghe Be-U deposit (modified after Wang et al., 2012; Zhang and Zhang, 2014).

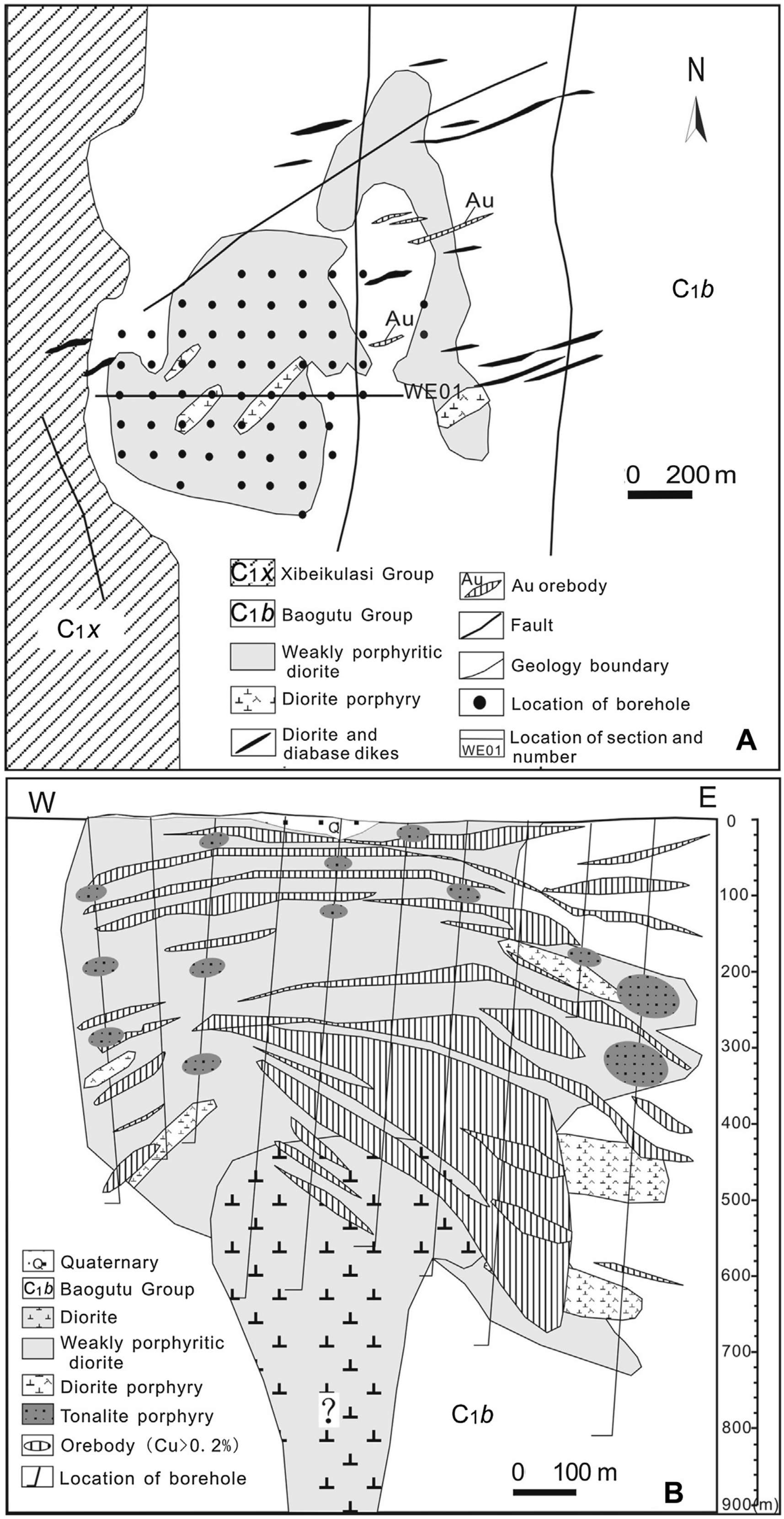

Figure 6. (A) Geological map of the Baogutu porphyry Cu deposit showing the intrusion complex. Line WE01 shows the location of the section shown in Fig. 6B, dots indicate the position of drill holes. (B) Geologic cross section along WE01 showing the host rocks to the Baogutu deposit and the copper ore bodies (Shen and Pan, 2013).

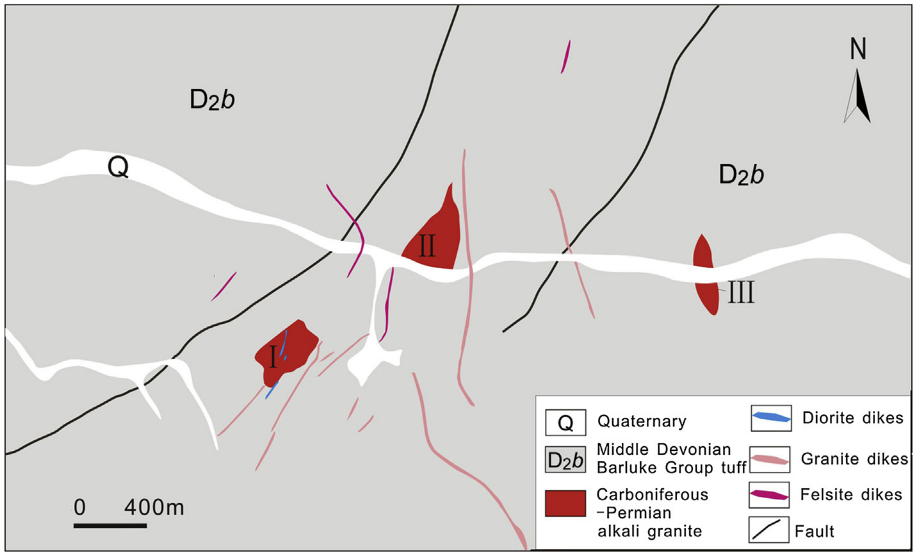

Figure 7. Schematic geological map of the Suyunhe Mo(-W) deposit (modified from local geological team, 2013).

4.7. *Late Carboniferous–early Permian porphyry-greisen Mo(-W) deposit*

Newly-discovered Mo(-W) and Mo deposits, located in the southern part of the West Junggar (Fig. 1B), are the Suyunhe Mo(-W) and Hongyuan Mo deposits. They could be the porphyry-greisen deposits based on the potassic alteration and extensive greisenization alteration as well as the dominant vein stockworks and lesser disseminated mineralization.

The Suyunhe Mo(-W) deposit lies about 80 km southeast of Yumin town (Fig. 1B). It has been explored by the local geological team. About 0.27 Mt Mo metal at an average grade of 0.032–0.716% have been obtained by the local geological team (Table 1). Fossil-dated Devonian strata (BGMRXUAR, 1993) occur widely in the Suyunhe area. They are the volcano-sedimentary strata of the middle Devonian Barluk Group composed of siltstone, tuff, and minor basalt. The Barluk Group is intruded by Carboniferous–Permian intrusions. Three mineralized intrusive stocks at Suyunhe have been recognized by the local geological team. They are the Suyunhe I, II, and III stocks, of which the Suyunhe I stock is the most important ore-bearing stock (Fig. 7). These stocks comprise plagiogranite porphyry and granite. The bulk of the Mo(-W) mineralization at Suyunhe occurred in the granite stocks and the wall rocks (Fig. 8A–D). The latter includes the tuff and tuffaceous siltstone of the Barluk Group. Associated hydrothermal alteration consists of potassic (K-feldspar) alteration and greisen (quartz-muscovite) occurring in the granite and the wall rocks.

The orebodies have vein and lenticular forms and have no distinct boundaries with country rocks, showing gradational contact relationships. The orebodies occupy an area of 3200 m × 600 m and extend to a depth 500 m. The ore types are dominant Mo ore and minor W and Mo-W ores. The dominant types of ore mineral assemblage are quartz-molybdenite (Fig. 8C), quartz-molybdenite-scheelite, and quartz-scheelite (Fig. 8D). The lesser amounts of disseminated mineralization (Fig. 8B) and dominant vein stockworks (Fig. 8A, C, D) occur in Suyunhe. Ore minerals mainly include molybdenite, scheelite, and minor chalcopyrite and pyrite. The gangue minerals are mainly quartz, muscovite, sericite, and calcite.

The Hongyuan Mo deposit or occurrence lies about 15 km north of Kelamay City and is under exploration. The early Carboniferous Tailegula Group occurs in the Hongyuan area and is composed of tuff and tuffaceous siltstone intercalated with basic volcanic rocks, with intrusions that include Kelamay granite pluton and Hongyuan granite stock (Fig. 9). The Hongyuan granite stock is associated with Mo mineralization (Li et al., 2012).

The Hongyuan granite stock consists of granite and porphyritic granite. Associated hydrothermal alteration consists of greisenization (Fig. 8E), tourmaline, and sericite alterations occurring in the granite stock (Yan et al., 2014). The dominant vein stockworks (Fig. 8F, G) and minor disseminated mineralization (Fig. 8H) occurred in the granite stock. A lot of quartz-muscovite veins and quartz-sulfide veins occur in the fissures of the granite (Fig. 8F, I). The quartz-sulfide veins include molybdenite-quartz, molybdenite-chalcopyrite-quartz, and chalcopyrite-pyrite-quartz veins (Fig. 8F, G, I). The mineral assemblages are dominant molybdenite and minor chalcopyrite and pyrite. Gangue minerals are quartz, muscovite, sericite, and tourmaline.

4.8. *Late Carboniferous–early Permian orogenic gold deposit*

Most of the gold deposits in the West Junggar region occur in the Hatu area within a zone about 70 km long and 20 km wide (Shen et al., 1993), on the northwest side of the Dalabute fault (Fig. 1B). The Hatu area mainly includes the Hatu (also named Qiqiu 1), Qiqiu 2, Lukeyi, Gezhitoug, Gezhigou, Huilushan, and Mandongshan gold deposits. The Hatu gold deposit is the largest. A total resource of about 56 tonnes at an average grade of 4.99 g/t has been reported in this deposit (Xiao et al., 2010a,b, Table 1), making it is the largest gold deposits in Xinjiang.

The Hatu Au mineralization is hosted in quartz veins and altered rocks emplaced within Carboniferous volcanic rocks (basalt and tuff) and sedimentary rocks (siltstone and sandstone). The Hatu area is characterized by a series of ENE-trending faults including the Hatu and Anqi faults, although NE, NW, and NS-trending structures are also present. Orebodies are spatially associated with the NE and NW-trending faults (Fig. 10). ENE and NS-trending faults are either not mineralized or contain uneconomic mineralization (Xiao et al., 2010b).

In the Hatu gold deposit, there are two types of ore: (1) quartz-veins (Fig. 11A), including quartz-calcite and quartz-sericite-pyrite-arsenopyrite veins; (2) altered rocks (Fig. 11B) including calcite, chlorite, and sericite altered rocks. The quartz-vein gold ores extend down dip to 400 m below the surface. Since 2006, the altered-rock gold ores have been found in deposits and extend

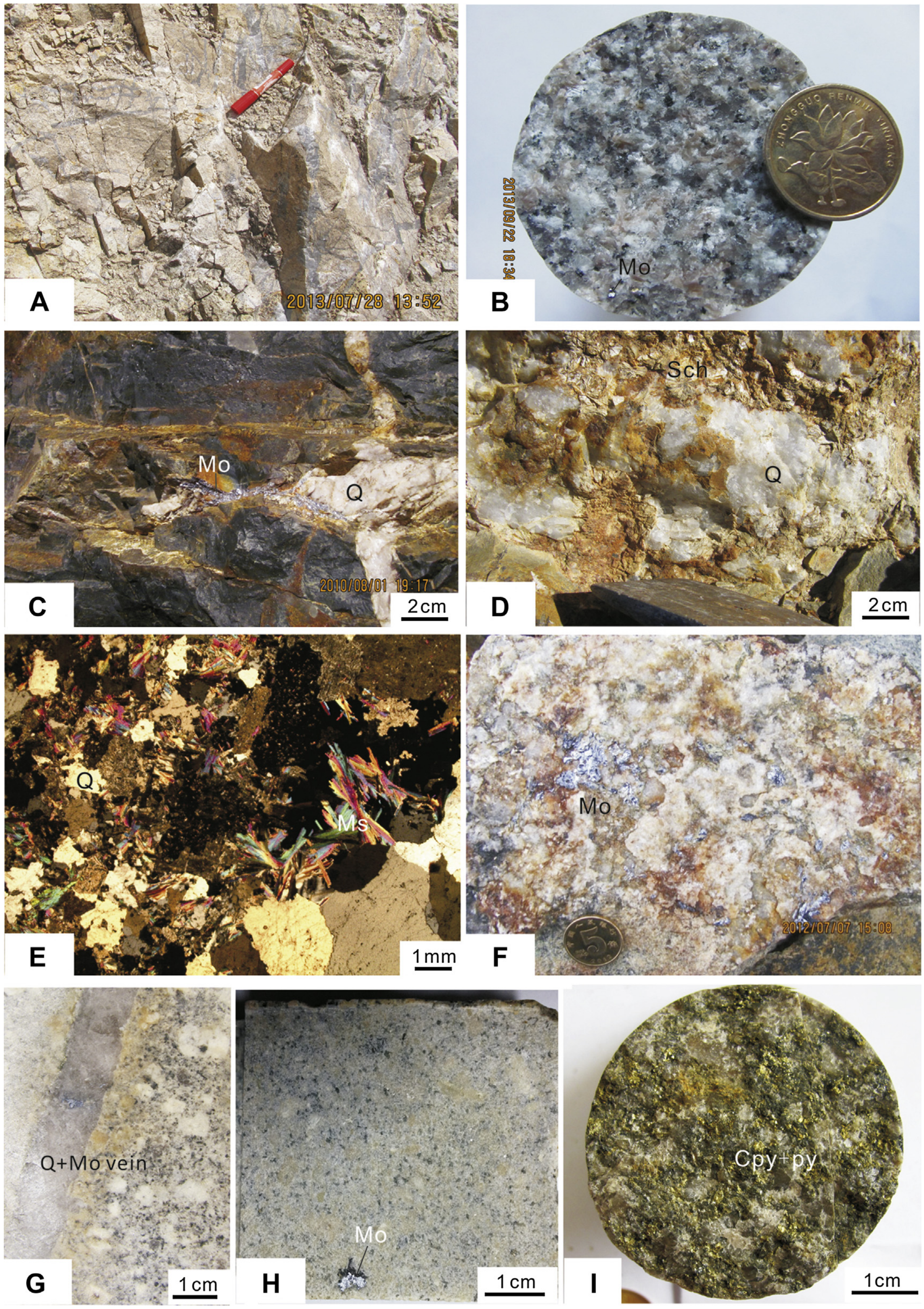

Figure 8. Photographs of the main ores from the Suyunhe Mo(-W) deposit and Hongyuan Mo deposit. Suyunhe Mo(-W) deposit: (A) quartz stockworks in granite; (B) disseminated molybdenite in granite; (C) quartz-molybdenite vein in tuff; (D) quartz-scheelite vein in tuff. Hongyuan Mo deposit: (E) greisenisation alteration in granite; (F) molybdenite occur in the fissures of the granite; (G) quartz- molybdenite vein in granite; (H) disseminated molybdenite in granite; (I) quartz-chalcopyrite-pyrite occur in the fissures of the granite. All photographs under nature lights excepting for E under transmitted lights. Abbreviations: Q: quartz; Ms: muscovite; Mo: molybdenite; Sch: scheelite; Cpy: chalcopyrite; Py: pyrite.

down dip from 400 to 1200 m below the surface (Xiao et al., 2010b). Thirty gold orebodies have been found, the largest of which is 800 m long and 4.23 m wide, extending down dip to 700 m below surface. The ore grades range from 2 to 300 g/t Au (average 5 g/t).

Minor quantities of sulphides (<3–5%) are present in the ores and include mainly pyrite, arsenopyrite, and secondary pyrrhotite, chalcopyrite, and tetrahedrite, with minor galena and sphalerite. Hydrothermal alteration haloes are not well developed, but where

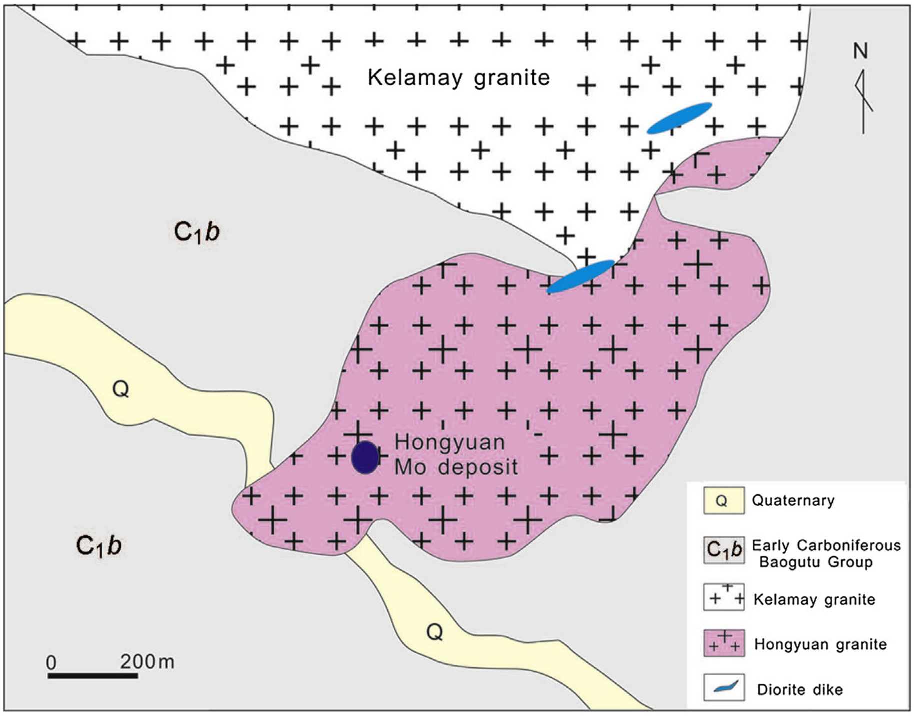

Figure 9. Schematic geological map of the Hongyuan Mo deposit (modified from local geological team, 2013).

present they contain carbonate, chlorite, sericite, quartz, and sulphides (Fig. 11C, D) with carbonate-sericite-chlorite–sulfide alteration assemblages. Most inclusions in quartz are rich in CO_2 (Wang et al., 2005).

Rui et al. (2002) interpreted the Hatu gold deposit as clearly being a structurally controlled orogenic gold deposit. We have added some evidence including the low sulfide volume (Fig. 11A, B), carbonate-sericite-chlorite-sulfide alteration assemblages in the host basalts (Fig. 11C, D), CO_2-rich ore fluids, and a spatial association with shear structures (Fig. 11B).

5. Discussion

5.1. Metallogenic ages

For comparison, Table 1 lists the available U-Pb zircon ages or whole rock Rb-Sr ages of the host rocks and Re-Os ages of molybdenites, ^{40}Ar-^{39}Ar ages, and Rb-Sr ages of fluid inclusions from quartz in the West Junggar region.

5.1.1. Ages of the Saur belt

In the Saur belt, the Kuoerzhenkuola epithermal gold deposit is hosted in volcanic-subvolcanic rocks with an age of 343 ± 22 Ma (Liu et al., 2003). Two ^{40}Ar-^{39}Ar ages from fluid inclusions also from auriferous quartz vein are 332 ± 22 Ma (Shen et al., 2007, 2008). Therefore, the epithermal gold mineralization event in the Saur Mountains occurred in the early Carboniferous Period.

5.1.2. Ages of the Xiemisitai-Sharburt belt

In the Xiemisitai-Sharburt belt, the Baiyanghe Be-U deposit occurred in the contact zone between the Baiyanghe granite porphyry and its wall rocks. The Baiyanghe granite porphyry has a zircon U-Pb age of 313.4 ± 2.3 Ma, suggesting that the Baiyanghe Be-U deposit may have formed in the late Carboniferous. The

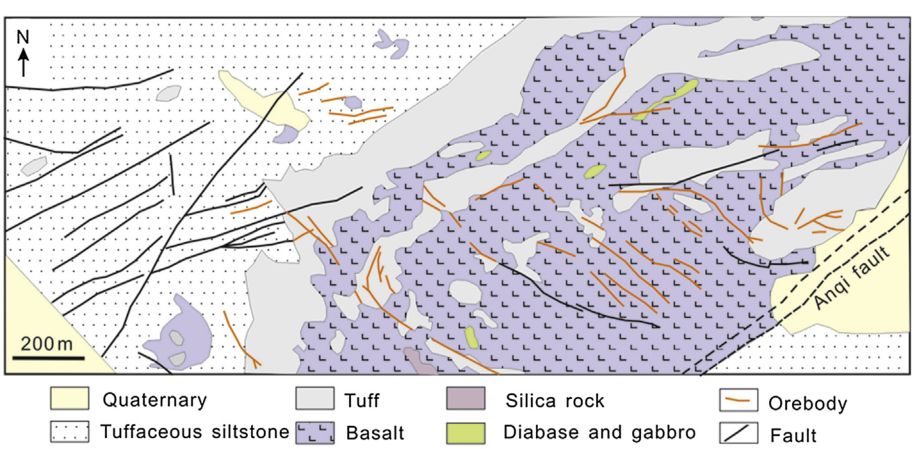

Figure 10. Schematic geological map of the Hatu Au deposit (modified from Shen et al., 1993; Xiao et al., 2010b; Zhu et al., 2013).

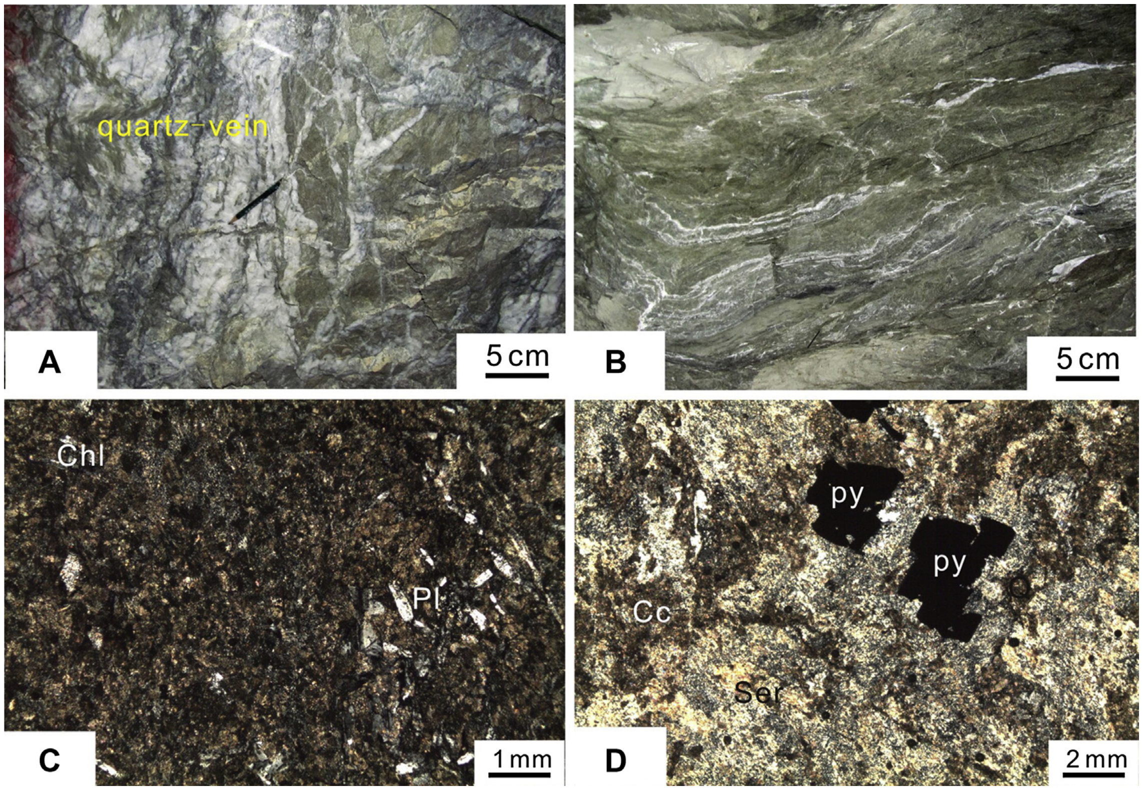

Figure 11. Photographs of the main ores and alterations from the Hatu Au deposit. (A) quartz-vein orebody; (B) altered-rock orebody; (C) calcite and chlorite alteration in basalt; (D) calcite, sericite, and pyrite alteration in basalt. A and B photographs under nature lights, C and D under transmitted lights. Abbreviations: Pl: plagioclase; Cc: calcite; Chl: chlorite; Ser: sericite; Py: pyrite.

Hongguleleng Cu-Zn deposit hosted in the mafic volcanic rocks of the fossil-dated middle Ordovician Bulukeqi Group indicated that the mineralization could not be earlier than middle Ordovician Period.

5.1.3. Ages of the Barluk-Kelamay belt

In the Barluk sub-belt, the SHRIMP zircon U-Pb ages of the main-stage diorites and late-stage diorite porphyry from the Jiamantieliek complex are 313 ± 4 Ma and 310 ± 5 Ma, respectively (Shen et al., 2013a). The average model age of molybdenites is 300.7 Ma for the Suyunhe W-Mo deposit (Shen et al., 2013b). Therefore, the Mo-W-Cu mineralization of the Barluk sub-belt could have taken place in the late Carboniferous–early Permian.

In the Kelamay sub-belt, the Sartuhai Chromite deposit is hosted in the Darbut ophiolite belt. In the Darbut ophiolite belt, the gabbro has a zircon U-Pb age of 391 ± 7 Ma (LA-ICP-MS) (Gu et al., 2009), and the basalts have an Rb-Sr isochron age of 411 ± 18 Ma (Li and Chen, 2004). The mineralization of the Sartuhai Cr deposit could be later than 391 ± 7 Ma.

At Bagutu, SIMS zircon U-Pb ages of the stage 1 diorites and stage 2 diorite porphyry from the Baogutu complex are 313.0 ± 2.2 and 312.3 ± 2.2 Ma, respectively (Shen et al., 2012b). Molybdenites separated from this deposit yielded Re-Os mean model ages of 310 ± 3.6 Ma (Song et al., 2007) and 312.4 ± 1.8 Ma (Shen et al., 2012b). The Hongyuan Mo deposit is hosted in the Hongyuan granite. A molybdenite Re-Os mean model age of 294 Ma was obtained (Li et al., 2012), while a molybdenite Re-Os isochron age was given as 314 ± 3.6 Ma (Yan et al., 2014). The Kuogesay gold deposit is hosted in the tuff of the Baogutu Group. The Kuogesay gold deposit is associated with the Baogutu IV diorite, which has a zircon U-Pb age of 309.9 ± 1.9 Ma (LA-ICP-MS) (Tang et al., 2009). An Rb-Sr isochron age was obtained of 311 ± 10 Ma from fluid inclusions from auriferous quartz vein (Li et al., 2000).

The Hatu gold deposit and Qiqiu 2 are hosted in the basalts and tuffs of the Tailegula Group. The Rb-Sr isochron age of the basalt of the Tailegula Group from the Hatu belt is 328 ± 31Ma (Li and Chen, 2004) and two SIMS zircon U-Pb ages of the tuffs from the Hatu belt were 324.0 ± 2.8 and 324.9 ± 3.4 Ma (Shen et al., 2013c), suggesting that the mineralization could not have been earlier than 324 Ma. This interpretation is supported by the Rb-Sr isochron ages of 290 ± 6.5 (Hatu) and 289 ± 29 Ma (Qiqiu 2) from fluid inclusions from auriferous quartz vein (Li et al., 2000). Therefore, the Au mineralization of the Hatu belt may have taken place in the early Permian.

Based on the available data, five epochs of ore formation in the West Junggar region can be recognized: (1) middle Ordovician VMS Cu-Zn; (2) Devonian podiform chromite; (3) early Carboniferous epithermal Au; (4) late Carboniferous granite-related Be-U, porphyry Cu and hydrothermal quartz vein Au; and (5) late Carboniferous to early Permian granite-related Mo(-W) and orogenic Au mineralization events. In particular, the development of mineralization reached a climax between the late Carboniferous and early Permian periods and is thought to have resulted from the extensive convective circulation of hydrothermal fluids and been associated with granitic intrusions.

5.2. Tectonic evolution and related mineralization

The West Junggar region is well endowed with a range of mineral deposit styles. Each of these styles is associated with the tectonics prevalent during their formation. Our previous study (Shen et al., 1993; Windley et al., 2007; Shen et al., 2008, 2009, 2012a,b, 2013a, 2014), together with other researches (e.g. Wang et al., 2004; Xiao et al., 2008, 2009, 2010a,b; Zhou et al., 2008; Geng et al., 2009, 2011; Tang et al., 2009, 2010; Zhang et al., 2011; Xiao et al., 2013; Kröner et al., 2014; Xiao and Santosh, 2014; Zhang and Zhang, 2014) suggested the following geodynamic evolution and associated mineralization of the West Junggar region. Plausible scenarios that attempt to explain the geodynamics of the West Junggar region, taking into account the context of associated mineralization are shown in Fig. 12.

In the northern part of the West Junggar region, during the middle Ordovician and late Silurian, the Hongguleleng Ocean was subducted, forming the Sharburt and Xiemisitai arc volcanic rocks and associated VMS Cu-Zn mineralization (Fig. 12A; Shen et al., 2012a, 2014). During the Devonian and Carboniferous periods, subduction of the Irtysh-Zaysan oceanic plate resulted in a series of magmatic arc (Shen et al., 2008; Zhou et al., 2008; Guo et al., 2010) and back-arc basins (Zhang and Zhang, 2014) on the northern margin of the Sharburt and Xiemisitai arc (Fig. 12B). The epithermal Au and porphyry Cu deposits occurred in the early Carboniferous volcanic complexes and intrusions, respectively (Shen et al., 2007, 2008; Guo et al., 2010), while the granite-related Be-U deposit formed in the contact zone between late Carboniferous granite and its wall rocks (Wang et al., 2012; Zhang and Zhang, 2014).

In the southern part of the West Junggar region, the Darbut ophiolite belt and associated Sartuhai chromite deposits formed in a Devonian back-arc basin (Fig. 12B, Zhang et al., 2011). Subduction along the Darbut fault was synchronous towards the north-west and south-east during the late Carboniferous, creating the Baogutu intra-oceanic arc in the southeastern Darbut fault and the Baobei intra-oceanic arc in the northwestern Darbut fault (Fig. 12C, Zhang et al., 2011; Shen et al., 2013c). Meanwhile, subduction along the Mayile fault was towards the northwest, forming the Barluk intra-oceanic arc in the northwestern Mayile Fault (Fig. 12C; Shen et al., 2013a). This geodynamic process led to the formation of subduction-related diorites and associated Cu and Au deposits in the southern West Junggar (Fig. 12C), represented by the Baogutu porphyry Cu deposit (Zhang et al., 2006; Song et al., 2007; Shen et al., 2009) and Kuogesay Au deposit (Shen et al., 1993; An and

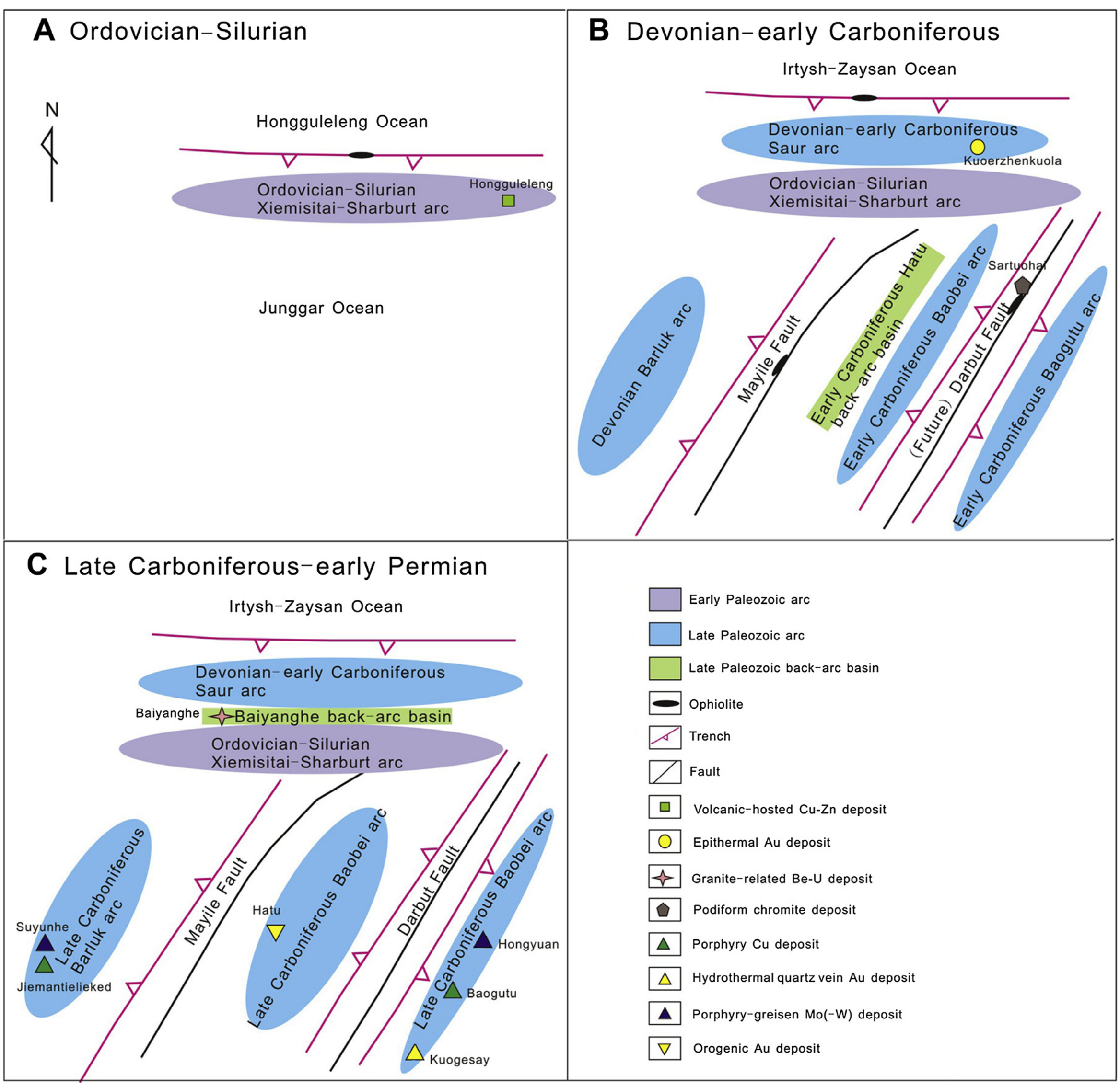

Figure 12. Proposed tectonic evolution and associated mineralization in the West Junggar region from Ordovician to Permian (data from Shen et al., 1993; Wang et al., 2004; Zhu and Xu, 2006; Shen et al., 2008, 2009, 2012, 2013a, 2014; Xiao et al., 2008, 2009, 2010a,b; Zhou et al., 2008; Geng et al., 2009, 2011; Tang et al., 2009, 2010; Yin et al., 2010; Zhang et al., 2011; Zhang and Zhang, 2014).

Zhu, 2010) in the Kelamay Region and the newly-discovered Jiamantieliek porphyry Cu deposits (Shen et al., 2013a) in the Barluk mountains. During the late Carboniferous to early Permian, subduction along the Darbut Fault and Mayile Fault continued and this led to the formation of granites and associated Mo-W-Au deposits in the southern West Junggar, represented by the Suyunhe Mo(-W) deposit in the Barluk Mountains, and Honghuan Mo and Hatu Au deposits in the Kelamay region.

6. Conclusions

1. The West Junggar region has developed three metallogenic belts from north to south: (1) late Paleozoic Saur Au-Cu belt, (2) early Paleozoic Xiemisitai-Sharburt Be-U-Cu-Zn belt, and (3) late Paleozoic Barluk-Kelamay Au-Cu-Mo-Cr belt.
2. Eight types of mineralization have been distinguished: (1) VMS Cu-Zn, (2) epithermal Au, (3) granite-related Be-U, (4) podiform Chromite, (5) porphyry Cu, (6) hydrothermal vein Au, (7) porphyry-greisen Mo(-W), and (8) orogenic Au deposits.
3. Five tectonic-mineralized epochs are recognized: (1) Ordovician subduction-related mafic magma and VMS Cu-Zn; (2) Devonian ophiolite and podiform Chromite; (3) early Carboniferous subduction-related intermediate magma and epithermal Au and porphyry Cu; (4) late Carboniferous subduction-related intermediate and felsic magma and porphyry Cu, hydrothermal vein Au, and granite-related Be-U; and (5) late Carboniferous to early Permian felsic magma and porphyry-greisen Mo(-W) and orogenic Au mineralization.

Acknowledgments

We are very grateful to Guest Editor Wenjiao Xiao, Editor-in-Chief M. Santosh and two reviewers for constructive comments and improvement of the manuscript. Thanks are given to Xinjiang Geoexploration Bureau of Nonferrous Metals and Xinjiang Bureau of Geology and Mineral Exploration for working in field. This paper was financially supported by the Innovative Project of the Chinese Academy of Sciences (KZCX-EW-LY02), National Natural Science Foundation of China (Grant Nos. U1303293, 41390441, 41272109), and National 305 Project (2011BAB06B01).

References

An, F., Zhu, Y.F., 2010. Native antimony in the Baogutu gold deposit (west Junggar, NW China): its occurrence and origin. Ore Geology Reviews 37, 214–223.

BGMRXUAR (Bureau of Geology and Mineral Resources of Xinjiang Uygur Autonomous Region), 1993. Regional Geology of Xinjiang Uygur Autonomous Region. Geological Publishing House, Beijing, 841 pp (in Chinese with English abstract).

Chen, J.F., Han, B.F., Jia, J.Q., Zhang, L., Xu, Z., He, G.Q., Wang, T., 2010. Zircon U–Pb ages and tectonic implications of Paleozoic plutons in northern West Junggar, North Xinjiang, China. Lithos 115, 137–152.

Chen, B., Arakawa, Y., 2005. Elemental and Nd-Sr isotopic geochemistry of granitoids from the West Junggar foldbelt (NW China), with implications for Phanerozoic continental growth. Geochimica et Cosmochimica Acta 69, 1307–1320.

Chen, B., Jahn, B.M., 2004. Genesis of post-collisional granitoids and basement nature of the Junggar Terrane, NW China: Nd-Sr isotope and trace element evidence. Journal of Asian Earth Science 23, 691–703.

Geng, H.Y., Sun, M., Yuan, C., Xiao, W.J., Xian, W.S., Zhao, G.C., Zhang, L.F., Wong, K., Wu, F.Y., 2009. Geochemical, Sr–Nd and zircon U–Pb–Hf isotopic studies of late Carboniferous magmatism in the Western Junggar, Xinjiang: implications for ridge subduction? Chemical Geology 266, 364–389.

Geng, H.Y., Sun, M., Yuan, C., Zhao, G.C., Xiao, W.J., 2011. Geochemical and geochronological study of early Carboniferous volcanic rocks from the West Junggar: petrogenesis and tectonic implications. Journal of Asian Earth Sciences 42, 854–866.

Gu, P.Y., Li, Y.J., Zhang, B., Tong, L.L., Wang, J.N., 2009. LA-ICP-MS zircon U-Pb dating of gabbro in the Darbut ophiolite, western Junggar, China. Acta Petrologica Sinica 25 (6), 1364–1372 (in Chinese with English abstract).

Guo, Z.L., Li, J.X., Qin, K.Z., Dong, L.H., Guo, X.J., Tang, D.M., Du, X.W., 2010. Zircon U-Pb geochronology and geochemistry of Hanzheganeng Cu-Au deposit in West Junggar, Xinjiang: implications for magma source and metallogenic tec tonic setting. Acta Petrologica Sinica 26 (12), 3563–3578 (in Chinese with English abstract).

Han, B.F., Ji, J.Q., Song, B., Chen, L.H., Zhang, L., 2006. Late Paleozoic vertical growth of continental crust around the Junggar Basin, Xinjiang, China (Part I): timing of post-collisional plutonism. Acta Petrologica Sinica 22, 1077–1086 (in Chinese with English abstract).

Hu, A.Q., Jahn, B.M., Zhang, Y., 2000. Crustal evolution and Phanerozoic crustal growth in northern Xinjiang: Nd isotopic evidence. Part I. Isotopic characterization of basement rocks. Tectonophysics 328, 15–52.

Jahn, B.M., Wu, F., Chen, B., 2000. Granitoids of the Central Asian Orogenic Belt and continental growth in the Phanerozoic. Transactions of the Royal Society of Edinburgh Earth Sciences 91, 181–193.

Jahn, B.M., Windley, B., Natal'in, B., Dobretsov, N., 2004. Phanerozoic continental growth in Central Asia. Journal of Asian Earth Sciences 23, 599–603.

Kröner, A., Kovach, V., Belousova, E., Hegner, E., Armstrong, R., Dolgopolova, A., Seltmann, R., Alexeiev, D.V., Hoffmann, J.E., Wong, J., Sun, M., Cai, K., Wang, T., Tong, Y., Wilde, S.A., Degtyarev, K.E., Rytsk, E., 2014. Reassessment of continental growth during the accretionary history of the Central Asian Orogenic Belt. Gondwana Research 25, 103–125.

Kröner, A., Alexeiev, D.V., Rojas-Agramonte, Y., Hegner, E., Wong, J., Xia, X., Belousova, E., Mikolaichuk, A.V., Seltmann, R., Liu, D., Kiselev, V.V., 2013. Mesoproterozoic (Grenvilleage) terranes in the Kyrgyz North Tianshan: zircon ages and Nd–Hf isotopic constraints on the origin and evolution of basement blocks in the southern Central Asian Orogen. Gondwana Research 23, 272–295.

Li, H.Q., Chen, F.W., Cai, H., 2000. Study on Rb-Sr isotopie ages of gold deposits in West Junggar area, Xinjiang. Acta Geologica Sinica 72, 181–192 (in Chinese with English abstract).

Li, H.Q., Chen, F.W., 2004. Isotopic Geochronology of Regional Mineralization in Xinjiang, China. Geological Publishing House, Beijing, pp. 19–42 (in Chinese with English abstract).

Li, Y.J., Wang, R., Wei, D., Tong, L.L., Zhang, B., Yang, G.X., Wang, J.N., Zhao, Y.M., 2012. Discovery of the porphyry copper-molybdenum deposits and prospecting reflections in southern Darbut tectonic magmatic belts, West Junggar, China. Acta Petrologica Sinica 28, 2009–2014 (in Chinese with English abstract).

Liu, G.R., Long, Z.N., Chen, Q.Z., Zhou, G., 2003. The formation age and geochemical characteristics of volcanic rock of Kuoerzhenkuolas gold mine in Xinjiang. Xinjiang Geology 21 (2), 177–180 (in Chinese).

Pirajno, F., Seltmann, R., Yang, Y.Q., 2011. A review of mineral systems and associated tectonic settings of northern Xinjiang, NW China. Geoscience Frontiers 2 (2), 157–185.

Rui, Z.Y., Goldfarb, R.J., Qiu, Y.M., Zhou, T.H., Chen, R.Y., Pirajno, F., Yun, G., 2002. Paleozoic-early Mesozoic gold deposits of the Xinjiang Autonomous region, northwestern China. Mineralium Deposita 37, 393–418.

Santosh, M., Kusky, T., 2010. Origin of paired high pressure–ultrahigh-temperature orogens: a ridge subduction and slab window model. Terra Nova 22, 35–42.

Şengör, A.M.C., Natal'in, B.A., Burtman, U.S., 1993. Evolution of the Altaid tectonic collage and Paleozoic crustal growth in Eurasia. Nature 364, 209–304.

Shen, P., Shen, Y.C., Li, X.H., Pan, H.D., Zhu, H.P., Meng, L., Dai, H.W., 2012a. Northwestern Junggar Basin, Xiemisitai Mountains, China: a geochemical and geochronological approach. Lithos 140–141, 103–118.

Shen, P., Shen, Y.C., Liu, T.B., Li, G.M., Zeng, Q.D., 2007. Genesis of volcanic-hosted gold deposits in the Sawur gold belt, northern Xinjiang, China: evidence from REE, stable isotopes, and noble gas isotopes. Ore Geology Review 32, 207–226.

Shen, P., Shen, Y.C., Liu, T.B., Li, G.M., Zeng, Q.D., 2008. Geology and geochemistry of the early Carboniferous Eastern Sawur caldera complex and associated gold epithermal mineralization, Sawur Mountains, Xinjiang, China. Journal of Asian Earth Sciences 32, 259–279.

Shen, P., Shen, Y.C., Liu, T.B., Meng, L., Dai, H.W., Yang, Y.H., 2009. Geochemical signature of porphyries in the Baogutu porphyry copper belt, western Junggar, NW China. Gondwana Research 16, 227–242.

Shen, P., Shen, Y.C., Pan, H.D., Li, X.H., Dong, L.H., Wang, J.B., Zhu, H.P., Dai, H.W., Guan, W.N., 2012b. Geochronology and isotope geochemistry of the Baogutu porphyry copper deposit in the West Junggar region, Xinjiang, China. Journal of Asian Earth Sciences 49, 99–115.

Shen, P., Shen, Y.C., Pan, H.D., Wang, J.B., Zhang, R., Zhang, Y.X., 2010a. Baogutu Porphyry Cu-Mo-Au Deposit, West Junggar, Northwest China: petrology, alteration, and mineralization. Economic Geology 105, 947–970.

Shen, P., Shen, Y.C., Wang, J.B., Zhu, H.P., Wang, L.J., Meng, L., 2010b. Methane-rich fluid evolution of the Baogutu porphyry Cu-Mo-Au deposit, Xinjiang, NW China. Chemical Geology 275, 78–98.

Shen, P., Pan, H.D., Xiao, W.J., Shen, Y.C., 2014. An Ordovician intra-oceanic subduction system influenced by ridge subduction in the West Junggar, Northwest China. International Geology Review 56 (2), 206–223.

Shen, P., Xiao, W.J., Pan, H.D., et al., 2013a. Petrogenesis and tectonic settings of the Late Carboniferous Jiamantieliek and Baogutu ore-bearing porphyry intrusions in the southern West Junggar, NW China. Journal of Asian Earth Sciences 75, 158–173.

Shen, P., Pan, H.D., Xiao, W.J., et al., 2013b. Two geodynamic–metallogenic events in the Balkhash (Kazakhstan) and the West Junggar (China): Carboniferous porphyry Cu and Permian greisen W-Mo mineralization. International Geology Review 55 (13), 1660–1687.

Shen, P., Pan, H.D., Xiao, W.J., et al., 2013c. Early Carboniferous intra-oceanic arc and back-arc basin system in the West Junggar, NW China. International Geology Review 55 (16), 1991–2007.

Shen, P., Pan, H.D., 2013. Country-rock contamination of magmas associated with the Baogutu porphyry Cu deposit, Xinjiang, China. Lithos 177, 451–469.

Shen, Y.C., Jin, C.W., Qi, J.Y., 1993. Ore- Forming Model and Mechanism of Gold Mineralization Area in West Junggar. In: Guangchi, Tu (Ed.), New Developments of Solid Earth Sciences of Northern Xinjiang. Science Press, Beijing pp.137–150 (in Chinese).

Song, H.X., Liu, Y.L., Qu, W.J., Song, B., Zhang, R., Cheng, Y., 2007. Geological characters of Baogutu porphyry copper deposit in Xinjiang, NW China. Acta Petrologica Sinica 23, 1891–1988 (in Chinese with English abstract).

Tan, J.J., Zhu, Y.F., 2010. Study on Fe-Ni-As-S mineral assemblages in Sartohay chromite deposit, Xinjiang, China. Acta Petrologica Sinica 26 (8), 2264–2274 (in Chinese with English abstract).

Tang, G.J., Wang, Q., Wyman, D.A., Li, Z.X., Zhao, Z.H., Jia, X.H., Jiang, Z.Q., 2010. Ridge subduction and crustal growth in the Central Asian Orogenic Belt: evidence from Late Carboniferous adakites and high-Mg diorites in the western Junggar region, northern Xinjiang (west China). Chemical Geology 277, 281–300.

Tang, G.J., Wang, Q., Zhao, Z.H., Derek, A.W., Chen, H.H., Jia, X.H., Jiang, Z.Q., 2009. Geochronology and geochemistry of the ore-bearing porphyries in Baogutu area (Western Junggar): petrogenesis and their implications for tectonics and Cu-Au mineralization. Earth Science—Journal of China University of Geosciences 34, 56–74 (in Chinese with English abstract).

Wang, L.J., Wang, J.B., Wang, Y.W., Zhu, H.P., 2006. S, Pb, C isotopes geochemistry from gold deposits in Junggar-East Tianshan Mountains area and the indication for gold mineralization, North Xinjiang. Acta Petrologica Sinica 22 (5), 1437–1447 (in Chinese with English abstract).

Wang, L.J., Wang, J.B., Wang, Y.W., Zhu, H.P., Qu, L.L., 2005. The study of ore-fluid and C-S-Pb isotope of S-rich and S-poor type epithermal gold deposits, Junggar area, Xinjiang. Acta Petrologica Sinica 21, 1382–1388 (in Chinese with English abstract).

Wang, J.B., Wang, Y.W., Wang, L.J., 2004. The Junggar immature continental crust province and its mineralization. Acta Geologica Sinica 78, 337–344 (in Chinese with English abstract).

Wang, M., Li, X.F., Guo, W., Li, Y.L., Shi, Z.L., Lu, K.G., 2012. Geological characteristics of Baiyanghe Beryllium-Uranium deposits in Xuemisitan volcanic belt, Xinjiang. Mineral Exploration 3, 34–40 (in Chinese with English abstract).

Wang, R., Zhu, Y.F., 2007. Geology of Baobei gold deposit in western Junggar and zircon SHRIMP age of its wall-rock, Western Junggar (Xinjiang, NW China). Geological Journal of China University 13, 590–602 (in Chinese with English abstract).

Wei, S.N., Zhu, Y.F., 2010. Emplacement of the intermediate and acid magmatic rocks in Xinjiang: constraints from the P-T-fO_2 and geochemistry. Acta Geologica Sinica 84, 1017–1029.

Windley, B.F., Alexeiev, D., Xiao, W.J., Kröner, A., Badarch, G., 2007. Tectonic models for accretion of the Central Asian Orogenic Belt. Journal of the Geological Society of London 164, 31–47.

Xiao, F., Xu, C.Y., Zhang, F.J., Lin, C.X., 2010a. Major breakthrough in the Hatu gold deposit, Western Junggar, XinJiang. Xinjiang Geology, 409–412 (in Chinese with English abstract).

Xiao, W.J., Han, C.M., Yuan, C., Sun, M., Shoufa, L., Chen, H.L., Li, Z.L., Li, J.L., Sun, S., 2008. Middle Cambrian to Permian subduction-related accretionary orogenesis of Northern Xinjiang, NW China: Implications for the tectonic evolution of central Asia. Journal of Asian Earth Sciences 32, 102–117.

Xiao, W.J., Huang, B.C., Han, C.M., Sun, S., Li, J.L., 2010b. A review of the western part of the Altaids: a key to understanding the architecture of accretionary orogens. Gondwana Research 18, 253–273.

Xiao, W.J., Kröner, A., Windley, B.F., 2009. Geodynamic evolution of Central Asia in the Paleozoic and Mesozoic. International Journal of Earth Sciences 98, 1185–1188.

Xiao, W.J., Santosh, M., 2014. The western Central Asian Orogenic Belt: a window to accretionary orogenesis and continental growth. Gondwana Research 25, 1429–1444.

Xiao, W.J., Windley, B.F., Allen, M.B., Han, C.M., 2013. Paleozoic multiple accretionary and collisional tectonics of the Chinese Tianshan orogenic collage. Gondwana Research 23, 1316–1341.

Yuan, F., Zhou, T.F., Tan, L.G., Fan, Y., Yang, W.P., He, L.X., Yue, S.C., 2006. Isotopic ages of the I-type granites in West Junggar Sawuer region. Acta Petrologica Sinica 22 (5), 1238–1248 (in Chinese with English abstract).

Yan, Y.H., Shen, P., Pan, H.D., Wang, J.N., Zhong, S.H., Liu, X.G., 2014. Research on the fluid inclusion and Re-Os dating of Hongyuan Mo deposit and Tuketuke Mo-Cu deposit, West Junggar, Xinjiang. Chinese Journal of Geology 49 (1), 287–304 (in Chinese with English abstract).

Yang, G.X., Li, Y.J., Gu, P.Y., Yang, B.K., Tong, L.L., Zhang, H.W., 2012. Geochronological and geochemical study of the Darbut Ophiolitic Complex in the West Junggar (NW China): implications for petrogenesis and tectonic evolution. Gondwana Research 21, 1037–1049. http://dx.doi.org/10.1016/j.gr.2011.07.029.

Yin, J.Y., Yuan, C., Sun, M., Long, X.P., Zhao, G.C., Wong, K.P., Geng, H.Y., Cai, K.D., 2010. Late Carboniferous high-Mg dioritic dikes in Western Junggar, NW China: geochemical features, petrogenesis and tectonic implications. Gondwana Research 17, 145–152.

Yin, Y.Q., Li, J.X., Chen, D.J., 2009. Gold Geology of the Northern Margin of Junggar Basin, Xinjiang. Chemical Industry Press, Beijing, pp. 1–356 (in Chinese).

Zhang, J., Xu, H.S., Wang, D.H., Zhang, Z.H., Chen, Z.Y., Zhang, R.M., 2009. Alteration characteristics of ore-forming Cr-spinel in the Sartokay chromite ore district, Xinjiang. Acta Geoscientica Sinica 30, 599–606 (in Chinese with English abstract).

Zhang, J.E., Xiao, W.J., Han, C.M., Mao, Q.G., Ao, S.J., Guo, Q.Q., Ma, C., 2011. A Devonian to Carboniferous intra-oceanic subduction system in Western Junggar, NW China. Lithos 125, 592–606.

Zhang, L.C., Wan, B., Jiao, X.I., Zhang, R., 2006. Characteristics and geological significance of adakitic rocks in copper-bearing porphyry in Baogutu, western Junggar. Geology in China 33, 626–631 (in Chinese with English abstract).

Zhang, X., Zhang, H., 2014. Geochronological, geochemical, and Sr-Nd-Hf isotopic studies of the Baiyanghe A-type granite porphyry in the Western Junggar: Implications for its petrogenesis and tectonic setting. Gondwana Research 25, 1554–1569.

Zhou, M.F., Robinson, P.T., Malpas, J., Aitchison, J., Sun, M., Bai, W.J., Hu, X.F., Yang, J.S., 2001. Melt/mantle interaction and melt evolution in the Sartohay high-Al chromite deposits of the Dalabute ophiolite (NW China). Journal of Asian Earth Sciences 19, 517–534.

Zhou, T.F., Yuan, F., Tan, L.G., Fan, Y., Yue, S.C., 2006. Geodynamic significance of the A-type granites in the Sawuer region in West Junggar, Xinjiang: rock geochemistry and SHRIMP zircon age evidence. Science in China (Series D) 49 (2), 113–123 (in Chinese with English abstract).

Zhou, T.F., Yuan, F., Fan, Y., Zhang, D.Y., Cooke, D., Zhao, G.C., 2008. Granites in the Saur region of the west Junggar, Xinjiang Province, China: geochronological and geochemical characteristics and their geodynamic significance. Lithos 106, 191–206.

Zhu, Y.F., An, F., Xu, C.Y., 2013. Hatu and its surrounding Au-Cu metallogenic regularity and prediction for deep ore prospecting in Xinjiang. Geological Publishing House, Beijing, p. 63 (in Chinese with English abstract).

Zhu, Y.F., Xu, X., 2006. The discovery of early Ordovian ophiolite mélange in Taerbahatai Mts., Xinjiang, NW China. Acta Petrologica Sinica 22, 2833–2842 (in Chinese with English abstract).